CrMn Underlayers for CoCrPt Thin Film Media

Li-Lien Lee
Intevac Inc., 3550 Bassett Street, Santa Clara, CA 95054
David E. Laughlin and David N. Lambeth
Data Storage Systems Center, Carnegie Mellon University, Pittsburgh, PA 15213

Abstract—**An improved CoCrPt thin film medium for longitudinal magnetic recording which has a coercivity significantly greater than prior CoCrPt thin film media was investigated. A CrMn alloy underlayer was used, instead of the conventional Cr underlayer. A coercivity value of 4280 Oe was easily reached in a CoCrPt film on a 50 nm thick CrMn underlayer as compared to 2810 Oe with a pure Cr underlayer. It was found that the coercivity increase due to the Mn addition was realized if the substrates were preheated before the sputtering. Grain boundary interdiffusion of Mn from the underlayer to the magnetic layer may be the cause for the coercivity increase.**

Index Terms—**Coercivity, CoCrPt, interdiffusion, CrMn, underlayer.**

I. Introduction

The ever increasing performance requirements for thin film hard disk magnetic media have motivated the use of new thin film layered structures and materials. Since the dramatic improvement of the in-plane coercivity of the Co alloy longitudinal media by Cr underlayers was discovered [1], researchers have investigated the role of the Cr underlayer and the deposition processes attempting to further improve the magnetic properties of the Co alloy thin film [2].

As the understanding of the role of the Cr underlayer progressed, it has been observed that the Cr underlayer can be further improved by alloying additions. Many substitutional alloying additions to the Cr underlayer have been investigated [3]. Lately, in order to induce a smaller grain size and to better promote epitaxial growth of the HCP structure in Pt containing Co alloys by adjusting the lattice parameter, the BCC Cr underlayers have been alloyed with V [4], Ti [5], or Mo [6]. In this study, we have investigated an alloy addition which does not change the lattice parameter of Cr. Nevertheless, a substantial increase in coercivity of the overlying Co alloy thin film was obtained.

Several factors make the addition of Mn into Cr an interesting topic of study: 1) Cr can dissolve a large amount of Mn and still retain a BCC solid solution structure. The solubility of Mn in bulk BCC Cr at room temperature is estimated to be greater than 25 at% [7]. 2) The antiferromagnetic temperature of Cr is substantially increased from 38 °C with even small additions of Mn. 3) The atomic volume of Mn (0.01224 nm^3/atom) is only slightly larger than that of Cr (0.01200 nm^3/atom), hence, the lattice parameter of the alloy is virtually unchanged from that of pure Cr even with a 25 at% Mn content. 4) Mn is relatively insoluble in HCP Co but is soluble in FCC Co. The combination of these factors implies that CrMn has potential for use as an underlayer.

Manuscript received on October 17, 1997.
This work was supported by a grant from the DOE, #FG02-90-ER45423.

II. Experimental

All films were prepared by RF diode sputtering on 1-inch square Corning 7509 glass coupons. Targets were 3-inch in diameter and the target-to-substrate distance was 1.2 inch. The base pressure before the deposition was $5x10^{-7}$ Torr or less and the sputtering Ar gas pressure was 10 mTorr. Deposition was performed at a fixed AC power of 100 watts (2.3 W/cm^2).

The CoCrPt target was a CoCr alloy target with bonded Pt chips while the CrMn targets were pure Cr with bonded Mn chips. Film compositions were determined by inductively coupled plasma (ICP) analysis. Film textures were characterized by symmetric x-ray diffractometry θ-2θ scan with CuK_α radiation. The in-plane bulk magnetic properties of the thin films were measured by vibrating sample magnetometry (VSM). ΔM measurements were performed with a force gradient magnetometer.

III. Results and Discussions

The ICP analysis showed the composition of the CoCrPt film was 78.5 at% Co, 9 at% Cr and 12.5 at% Pt. Unless otherwise noted, the Mn content of the CrMn alloy film used in this study was 22 at% Mn. The in-plane coercivities of 40 nm thick CoCrPt films plotted against the Cr and CrMn underlayer's thickness are shown in Figures 1 and 2. The films considered for Fig. 1 were deposited without substrate preheating whereas those films used for Fig. 2 were deposited with a substrate preheating of 250 °C.

There is very little difference in the Hc values of the CoCrPt/Cr and CoCrPt/CrMn films when these films are deposited onto unheated substrates. However, significantly higher Hc values are observed for films with the CrMn underlayers than films with the Cr underlayers when glass substrates are preheated to 250 °C. The Hc values are at least

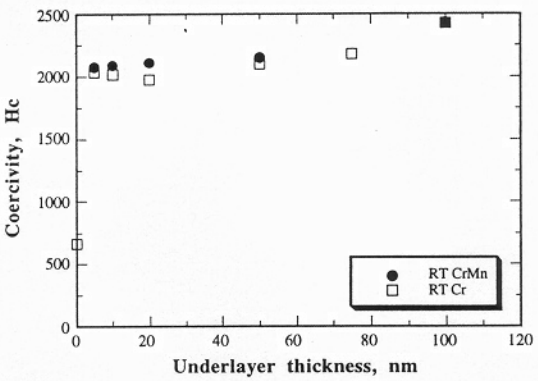

Fig. 1. In-plane coercivities of 40 nm thick CoCrPt films on CrMn and Cr underlayers of various thicknesses on glass substrates. No substrate preheating was used here.

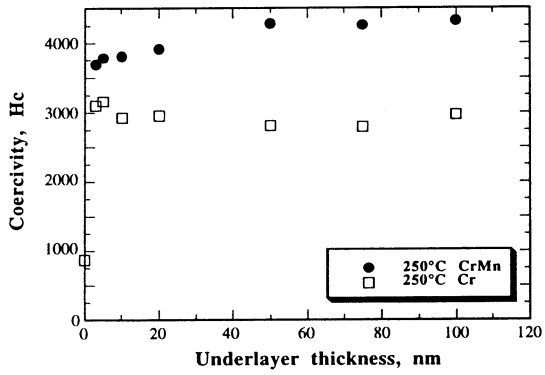

Fig. 2. In-plane coercivities of 40 nm thick CoCrPt films on CrMn and Cr underlayers of various thicknesses on glass substrates. Substrate preheating: 250 °C.

TABLE I
In-plane magnetic properties of 40 nm thick CoCrPt films on various thicknesses of CrMn underlayers. Substrate preheating: 250 °C.

CrMn thickness	Hc, Oe	S*	Mrt, memu/cm^2
100 nm	4315	0.90	0.87
75 nm	4258	0.88	0.84
50 nm	4280	0.89	0.88
20 nm	3913	0.89	0.95
10 nm	3808	0.89	0.97
5 nm	3782	0.89	1.06
3 nm	3695	0.89	1.06
0 nm	865	0.92	1.26

TABLE II
In-plane magnetic properties of 40 nm thick CoCrPt films on various thicknesses of Cr underlayers. Substrate preheating: 250 °C.

Cr thickness	Hc, Oe	S*	Mrt, memu/cm^2
100 nm	2961	0.77	0.93
75 nm	2792	0.78	0.82
50 nm	2810	0.82	0.91
20 nm	2953	0.85	0.99
10 nm	2952	0.86	1.03
5 nm	3162	0.88	1.05
3 nm	3092	0.88	1.11

25 % higher for all heated films with the CrMn underlayers than the corresponding films with the Cr underlayers. A maximum Hc of 4300 Oe was obtained with the CrMn underlayer as compared to 3200 Oe with the Cr underlayer. Table I and II list VSM measured in-plane bulk magnetic properties of the films shown in Fig. 2. In addition to the coercivity values, the coercive squareness values of the CoCrPt/CrMn films are also higher.

Selected x-ray θ-2θ scans of the films considered in Fig. 2 are plotted in Fig. 3 and 4 for comparison. The substrate heating induces (002) texture in both the Cr and the CrMn and the (002) diffraction peak becomes more pronounced as the film thickens. As anticipated, this (002) Cr or CrMn texture then induces the epitaxial growth of the (11$\bar{2}$0) CoCrPt texture. It is tempting to explain the higher coercivities of the CoCrPt films obtained on CrMn underlayers as due to increased (11$\bar{2}$0) textures of the films. However, it is observed that some of the films do not show stronger (11$\bar{2}$0) diffraction peaks but do show significantly higher coercivities. For example, compare the CoCrPt film

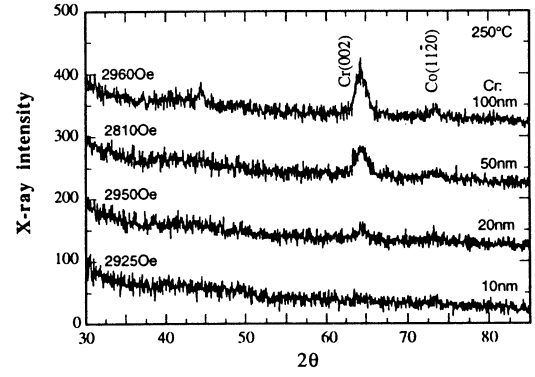

Fig. 3. X-ray diffraction spectra of 40 nm CoCrPt films on various thicknesses of Cr underlayers deposited on 250 °C preheated glass substrates.

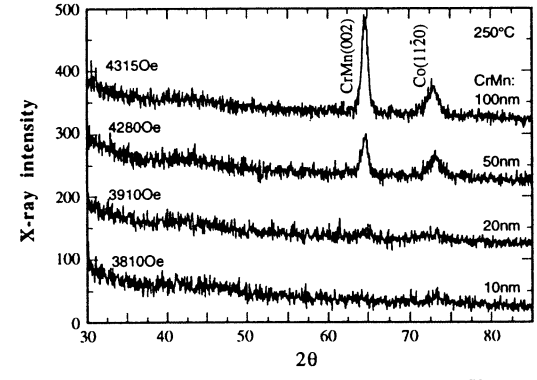

Fig. 4. X-ray diffraction spectra of 40 nm CoCrPt films on various thicknesses of CrMn underlayers deposited on 250 °C preheated glass substrates.

on 20 nm CrMn results to the CoCrPt film on 100 nm Cr results.

Previous studies showed that a MgO seed layer can induce strong (002) texture in a Cr underlayer film [8]. To see if a strong (002) textured CrMn underlayer can enhance coercivity, a CoCrPt(40nm)/CrMn(100nm) film was deposited without intentional heating onto a 12 nm thick MgO seed layer prepared on a glass substrate. Fig. 5 shows the x-ray θ-2θ scan of the specimen. It was found that although a much stronger (002) CrMn texture was obtained using this seed layer; the coercivity, 2884 Oe, of the film was low and the (11$\bar{2}$0) Co peak was not very strong. This indicates that the

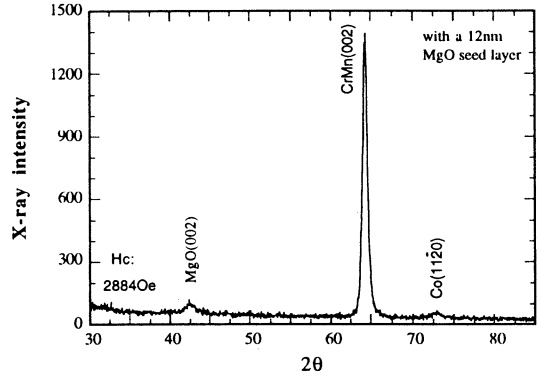

Fig. 5. X-ray θ-2θ scan of a CoCrPt(40 nm)/CrMn(100 nm) on a 12 nm thick MgO seed layer sputtered on a glass substrate without preheating.

TABLE III
In-plane magnetic properties of 40 nm thick CoCrPt films on 100 nm thick Cr and CrMn underlayers with and without a 2.5 nm thick intermediate layer.

Underlayer	CrMn		Cr	
Intermediate layer	no	Cr	no	CrMn
Hc, Oe	4315	3899	2961	3393
S*	0.90	0.88	0.77	0.82
Mrt, memu/cm^2	0.87	0.92	0.93	1.02

CrMn texture alone may not be the critical issue here. To achieve high coercivity CoCrPt films, the CrMn underlayers probably need to both exhibit a (002) texture and to be prepared at high temperature during the deposition of the CoCrPt films.

Very thin (2.5 nm) intermediate layers of Cr and CrMn deposited respectively between the CoCrPt/CrMn and CoCrPt/Cr films were used to study the interfacial chemistry effect. Table III lists the VSM measured in-plane magnetic properties of these films.

The coercivity and coercive squareness are always higher for CoCrPt films which are in contact with the CrMn. Because the inserted Cr and CrMn intermediate layers are thin and they have similar crystal structures and lattice constants, the CoCrPt/CrMn and CoCrPt/Cr film textures do not change by the insertion of intermediate layers. The magnetic property changes of the media due to the change of composition at the interface between the underlayer and the magnetic layer is probably caused by the interlayer diffusion of the Mn. This is consistent with the fact that substrate preheating enhances the coercivity increase of the CoCrPt/CrMn film and that substrate preheating is also known to accelerate the interdiffusion. If Mn atoms from the underlayer diffuse into potential FCC grain boundaries of the CoCrPt layer, or into the BCC Cr located at the CoCrPt grain boundaries preferentially over diffusion into the bulk of the CoCrPt grains, then this may magnetically separate the CoCrPt grains and increase the coercivity. It is conjectured that this grain-to-grain isolation or anti-ferromagnetic coupling may also result in a lower noise.

ΔM curves of 40 nm thick CoCrPt films on 50 nm Cr and CrMn underlayers are shown in Fig. 6. A positive peak in a ΔM plot reveals the existence of exchange coupling between the grains in the magnetic layer and its height is related to the degree of coupling [9]. Judging from Fig. 6, it is believed that the film with a CrMn underlayer has slightly less exchange coupling than the film with a Cr underlayer.

The effect of Mn concentration in the Cr alloy on coercivity has also been investigated. The Mn content of the CrMn underlayer was altered by adjusting the number of Mn chips on the Cr target to produce sputtered films with compositions 11 at% and 28 at% Mn. In-plane coercivities of 40 nm thick CoCrPt films are plotted in Fig. 7 versus the Mn contents of their underlayers. The coercivity increases with the Mn content and probably reaches its maximum between 11 and 28 at%. X-ray diffraction studies of the Cr-28 at% Mn film showed that the BCT α" phase had appeared in

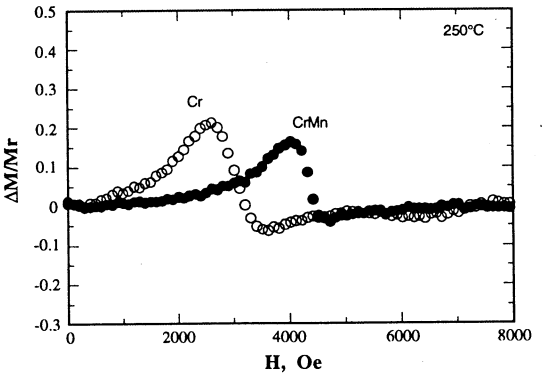

Fig. 6. ΔM plots of CoCrPt(40 nm) films on 50 nm thick Cr and CrMn underlayers.

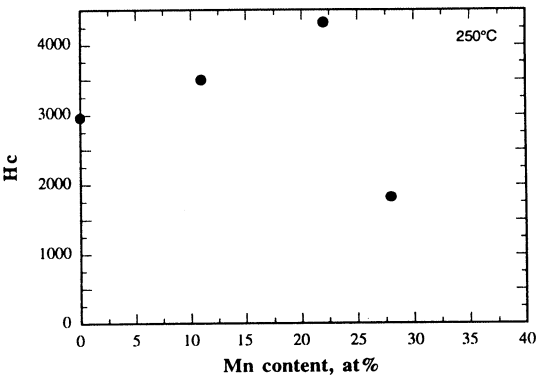

Fig. 7. Plot of the in-plane coercivity of a CoCrPt(40 nm) film vs. the Mn content of its CrMn underlayer.

the film. Therefore, we proposed that the highest Mn content of the CrMn underlayer that can be deposited which still remain in the BCC phase will probably result in the highest coercivity CoCrPt film.

IV. Conclusions

The use of CrMn underlayers can lead to higher coercivities in the overlying CoCrPt films than pure Cr underlayers. Substrate preheating during the deposition is necessary for the CrMn underlayer to induce high coercivity. Perhaps, interdiffusion of Mn from the underlayer to the grain boundaries of the magnetic layer alters the grain to grain isolation and results in a higher coercivity.

References

[1] J. P. Lazzari, I. Melnick and D. Randet, *IEEE Trans. Magn.*, vol. 3, pp. 205-207 (1967).
[2] J. Pressesky, S. Y. Lee, S. Duan and D. Williams, *J. Appl. Phys.*, vol. 69, pp. 5163-5165 (1991).
[3] N. Tani, M. Hashimoto, Y. Ishikawa, Y. Ota and K. Nakamura, *J. Appl. Phys.*, vol. 67, pp. 7507-7509 (1990).
[4] M. A. Parker, J. K. Howard, R. Ahlert and K. R. Coffey, *J. Appl. Phys.*, vol. 73, pp. 5660-5662 (1993).
[5] Y. Shiroishi, Y. Hosoe, A. Ishikawa, Y. Yashisa, Y. Sugita, H. Suzuki, Y. Ohno and M. Ohura, *J. Appl. Phys.*, vol. 73, pp. 5569-5571 (1993).
[6]I. Okamoto, T. Okuyama, K. Sato and M. Shinohara, AB-03, *INTERMAG '97 DIGEST* (1996).
[7] M. Venkatraman and J. P. Neumann, *Bulletin of Alloy Phase Diagram*, vol. 7, No. 5, pp. 457-459 (1986).
[8] L. -L. Lee, B. K. Cheong, D. E. Laughlin, and D. N. Lambeth, *Appl. Phys. Lett.*, vol. 67, pp. 3638-3640 (1995).
[9] M. El-Hilo, K. O'Grady, P. I. Mayo, R. W. Chantrell, I. L. Sanders, and J. K. Howard, *IEEE Trans. Magn.*, vol. 28, pp. 3282-3284 (1992).